

**Supporting Information for**  
**Solvent effects and Dynamic Averaging of the  $^{195}\text{Pt}$  NMR**  
**Shielding in Cisplatin Derivatives**

Lionel A. Truflandier,<sup>1</sup> Kiplangat Sutter,<sup>1</sup> and Jochen Autschbach<sup>1,2</sup>

*<sup>1</sup>Department of Chemistry*

*312 Natural Sciences Complex*

*State University of New York at Buffalo*

*Buffalo, NY 14260-3000, USA*

*<sup>2</sup>e-mail: jochena@buffalo.edu*

(Dated: December 2, 2010)

## S1. RADIAL DISTRIBUTION FUNCTION ANALYSIS

TABLE S1: Location of the first and second peak of the ligand–water RDFs calculated for the solvated cisplatin derivatives, along with the corresponding average interatomic distance  $\bar{r}$ , the integration radius  $r_{\text{int}}$  (in Å) and the coordination number  $n$ . The atoms labeled  $\text{O}_w$  and  $\text{H}_w$  refer to water molecules.

Complex	<i>cis</i> -Pt(NH <sub>3</sub> ) <sub>2</sub> Cl <sub>2</sub>		<i>cis</i> -Pt(NH <sub>3</sub> ) <sub>2</sub> Br <sub>2</sub>		<i>cis</i> -Pt(NH <sub>3</sub> ) <sub>2</sub> (OH)Cl		<i>cis</i> -Pt(NH <sub>3</sub> ) <sub>2</sub> (OH) <sub>2</sub>	
	X=Cl		X=Br		X=Cl		X=∅	
Peak	First	Second	First	Second	First	Second	First	Second
N⋯O <sub>w</sub>					N[Cl]–N[O] <sup>a</sup>	N[Cl]–N[O]		
$\bar{r}^b$	3.0*/3.4*	4.1	3.0	4.6*	3.0*–3.2*	3.8*–**	3.1*	3.8*
<i>r</i> <sub>int</sub>	3.2*/3.6*	4.8	3.5	5.3*	3.4*–3.6*	4.3*–**	3.4*	4.3*
<i>n</i>	1.9*/3.2*	7.1	2.5	13.0*	2.1*–2.9*	7.9*–**	2.3*	7.0*
NH⋯O <sub>w</sub>					N[Cl]–N[O]	N[Cl]–N[O]		
$\bar{r}$	1.9	3.5	2.0	3.5	2.0–2.0*	3.6–3.5*	2.1	3.5
<i>r</i> <sub>int</sub>	2.5	4.7	2.7	4.8	2.6–2.5*	4.2–3.9*	2.5	4.4
<i>n</i>	0.7	9.3	0.8	10.5	0.7–0.4*	7.0–4.4*	0.5	8.0
X⋯H <sub>w</sub>								
$\bar{r}$	2.3	4.1*	2.6	4.2*	2.3	**	n/a	
<i>r</i> <sub>int</sub>	2.9	4.6*	3.0	4.7*	2.7	**	n/a	
<i>n</i>	2.2	18.0*	2.1	18.0*	1.7	**	n/a	
X⋯O <sub>w</sub>								
$\bar{r}$	3.3	4.7	3.5*	**	3.3	5.3	n/a	
<i>r</i> <sub>int</sub>	3.7	5.5	3.8*	**	3.9	6.4	n/a	
<i>n</i>	2.6	17.0	2.4*	**	3.2	31.0	n/a	
O⋯H <sub>w</sub>								
$\bar{r}$	n/a		n/a		1.6	3.5	1.7	3.4
<i>r</i> <sub>int</sub>	n/a		n/a		2.5	4.2	2.3	4.5
<i>n</i>	n/a		n/a		2.0	13.0	1.6	17.0
O⋯O <sub>w</sub>								
$\bar{r}$	n/a		n/a		2.7	4.8	2.7	4.3
<i>r</i> <sub>int</sub>	n/a		n/a		3.5	5.5	3.2	5.0
<i>n</i>	n/a		n/a		2.8	18.0	2.0	12.5

<sup>a</sup>The RDFs have been deconvoluted with respect to the nitrogen in trans position of the chlorine and oxygen atoms.

<sup>b</sup>Asterisks indicate that the peak is not well defined. Two asterisks indicate that no peak can be identified.

TABLE S2: Comparison of selected average interatomic distances  $\bar{r}$ , and the corresponding coordination numbers  $n$ , calculated from the ligand–water RDFs of solvated cisplatin.

Method	CP-aiMD		Classical-MD	Monte-Carlo
	This work	Ref. [1]/[2]	Ref. [3]	Ref. [4]
<hr/>				
N $\cdots$ O <sub>w</sub>				
$\bar{r}$ (Å)	3.2*	3.0/–	2.8	2.9
$n$	3.2*	2.9/–	4.1	3.6
<hr/>				
NH $\cdots$ O <sub>w</sub>				
$\bar{r}$ (Å)	1.9	–/1.8	1.8	1.9
$n$	0.7	–/0.8	0.8	0.8
<hr/>				
Cl $\cdots$ O <sub>w</sub>				
$\bar{r}$ (Å)	3.3	3.2*/–	3.6	3.6
$n$	2.6	2.9*/–	10.0	6.8
<hr/>				
Cl $\cdots$ H <sub>w</sub>				
$\bar{r}$ (Å)	2.3	2.3/2.3	2.6	2.6
$n$	2.2	1.7/1.2	1.2	0.9
<hr/>				

TABLE S3: Selected structural parameters of the solvated cisplatin derivative complexes.

Complex		Distance (Å)		Angle (deg)	
		Pt–N	Pt–X	N–Pt–N	X–Pt–X
<i>cis</i> -Pt(NH <sub>3</sub> ) <sub>2</sub> Cl <sub>2</sub>	CP-aiMD <sup>a</sup>	2.09 ± 0.04	2.35 ± 0.03	90.4 ± 4.1	92.3 ± 4.3
	Previous work <sup>b</sup>	2.03 ± 0.03	2.32 ± 0.01	89 ± 2	94 ± 4
	COSMO <sup>c</sup>	2.06	2.35	89.7	92.9
<i>cis</i> -Pt(NH <sub>3</sub> ) <sub>2</sub> Br <sub>2</sub>	CP-aiMD	2.10 ± 0.04	2.48 ± 0.04	89.1 ± 3.6	91.4 ± 3.8
	COSMO	2.07	2.49	88.3	93.2
<i>cis</i> -Pt(NH <sub>3</sub> ) <sub>2</sub> (OH) <sub>2</sub>	CP-aiMD	2.09 ± 0.04	2.06 ± 0.032	91.9 ± 4.3	88.7 ± 4.3
	COSMO	2.07	2.04	92.6	87.2
		Pt–N	Pt–Cl	N–Pt–N'	Cl–Pt–O
		Pt–N'	Pt–O		
<i>cis</i> -Pt(NH <sub>3</sub> ) <sub>2</sub> (OH)Cl	CP-aiMD	2.06 ± 0.04	2.34 ± 0.05	90.8 ± 4.3	92.2 ± 4.2
		2.12 ± 0.04	2.07 ± 0.05		
	COSMO	2.06	2.35	91.2	91.8
		2.08	2.04		

<sup>a</sup>Mean angle and distance values along with the respective standard deviations from the CP-aiMD.

<sup>b</sup>Values extracted from a CP-aiMD performed on *cis*-Pt(NH<sub>3</sub>)<sub>2</sub>Cl<sub>2</sub> within a 35 water molecules box, using the BLYP exchange-correlation functional.<sup>2</sup>

<sup>c</sup>From scalar-ZORA optimized structures using the conductor-like screening model along with the PBE functional and ZORA-optimized TZ2P- and QZ4P-STO basis sets for the ligand atoms and Pt, respectively. Geometry optimizations were performed without spatial symmetry constraints and the nature of the stationary points was verified by calculations of vibrational frequencies.

TABLE S4: Location of the first and second peak of the Pt–O and Pt–H RDFs calculated for the solvated cisplatin and the corresponding bromine derivative.

Complex	<i>cis</i> -Pt(NH <sub>3</sub> ) <sub>2</sub> Cl <sub>2</sub>		<i>cis</i> -Pt(NH <sub>3</sub> ) <sub>2</sub> Br <sub>2</sub>	
Pt···O <sub>w</sub>	First peak	Second peak	First peak	Second peak
$\bar{r}$ (Å)	3.5	4.9	3.4	4.2*/4.5*/5.7*
$r_{\text{int}}$	3.7	5.7	3.7	4.9*/6.1*
$n$	1.0	19.0	0.8	8.0*/22*
Pt···H <sub>w</sub>				
$\bar{r}$ (Å)	2.5	–	2.5*	–
$r_{\text{int}}$	3.2	–	3.4*	–
$n$	1.2	–	1.7*	–

TABLE S5: Location of the first three peaks of the Pt–O and Pt–H RDFs calculated for the cisplatin hydroxyl derivatives.

Complex	<i>cis</i> -Pt(NH <sub>3</sub> ) <sub>2</sub> (OH)Cl			<i>cis</i> -Pt(NH <sub>3</sub> ) <sub>2</sub> (OH) <sub>2</sub>		
Pt···O <sub>w</sub>	First peak	Second peak	Third peak	First peak	Second peak	Third peak
$\bar{r}$ (Å)	3.3*	3.9	**	3.4*	4.2	5.6
$r_{\text{int}}$	3.4*	4.6	**	3.6*	4.9	6.4
$n$	0.6*	8.5	**	0.7*	10.0	30.0
Pt···H <sub>w</sub>						
$\bar{r}$ (Å)	2.4	3.1	4.8	2.3	3.2	4.9
$r_{\text{int}}$	2.7	3.6	5.7	2.7	3.7	5.7
$n$	0.6	5.3	36.0	0.6	4.9	40.0

## S2. VIBRATIONAL DENSITY OF STATES ANALYSIS

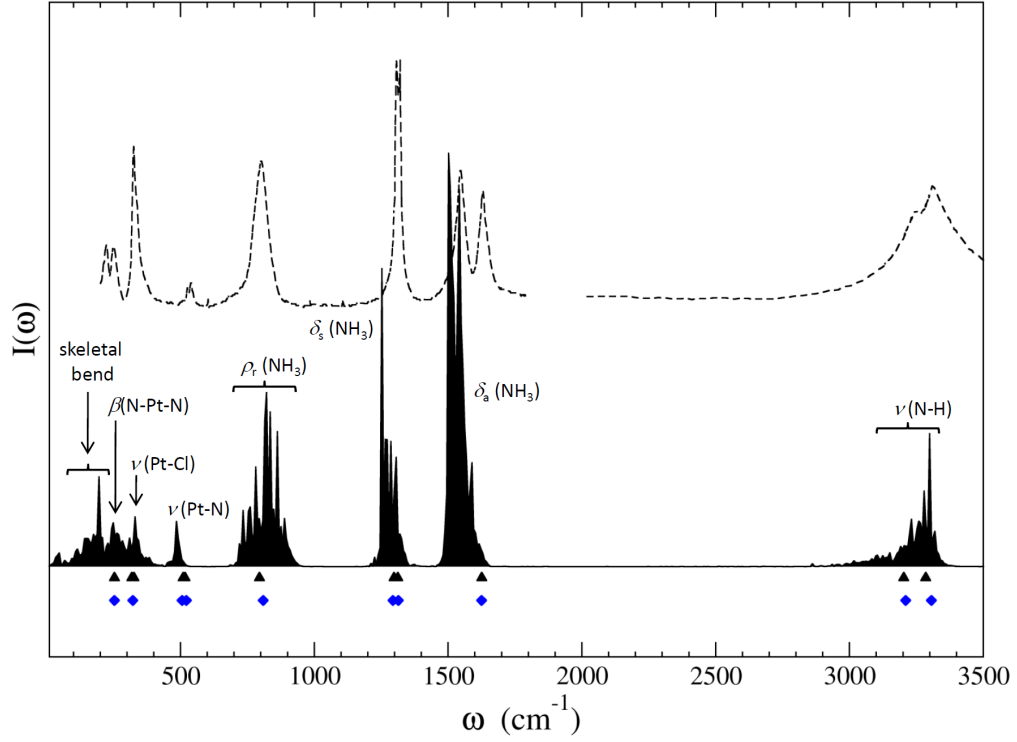


FIG. S1: CP-aiMD VDOS of the water-solvated *cis*-Pt(NH<sub>3</sub>)<sub>2</sub>Cl<sub>2</sub> system – isolated from the bulk water. For a qualitative comparison, the experimental IR spectrum of *cis*PtCl – solid sample dispersed in a KBr powder – has been reproduced from Ref. 5. Recent solid IR and Raman data<sup>6</sup> are also shown (black triangles and blue diamonds). The assignment of the vibrations is based on molecular quantum chemical calculations of Ref 6,7:  $\nu$ , stretching;  $\beta$ , in-plane bending;  $\delta_a$ , asymmetric deformation ;  $\delta_s$  symmetric deformation;  $\rho_r$ , rocking.

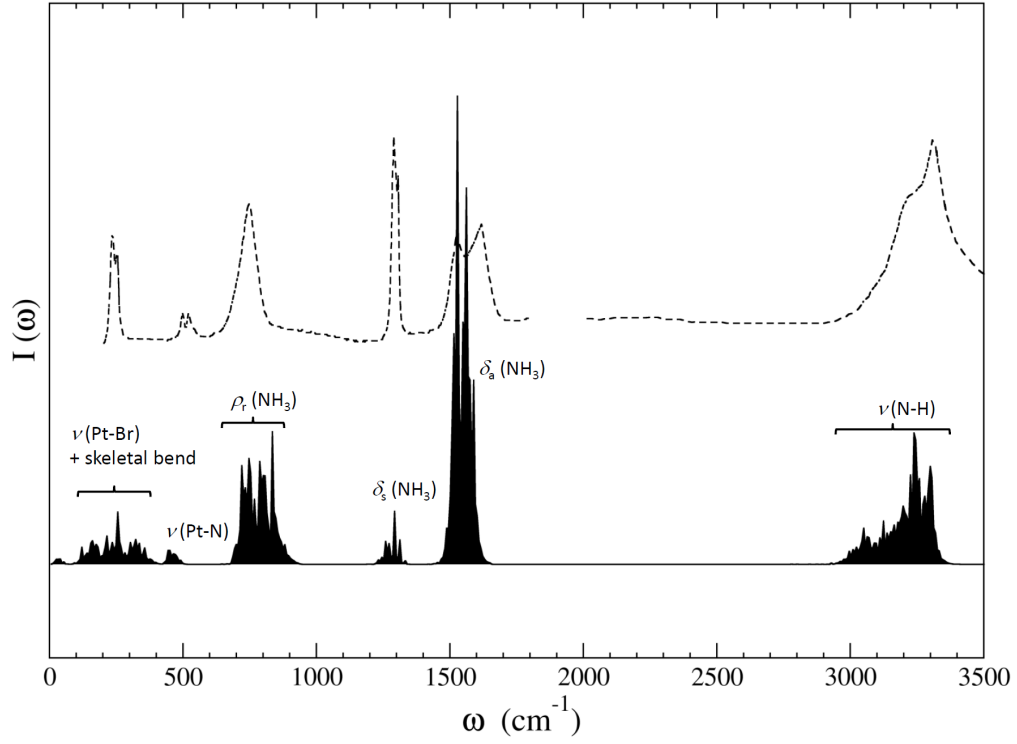


FIG. S2: CP-aiMD VDOS of the water-solvated *cis*-Pt(NH<sub>3</sub>)<sub>2</sub>Br<sub>2</sub> system – isolated from the bulk water. For a qualitative comparison, the experimental IR spectrum of cisPtBr – solid sample dispersed in a KBr powder – has been reproduced from Ref. 5. The assignment of the vibrations is based on molecular quantum chemical calculations performed as part of this work.

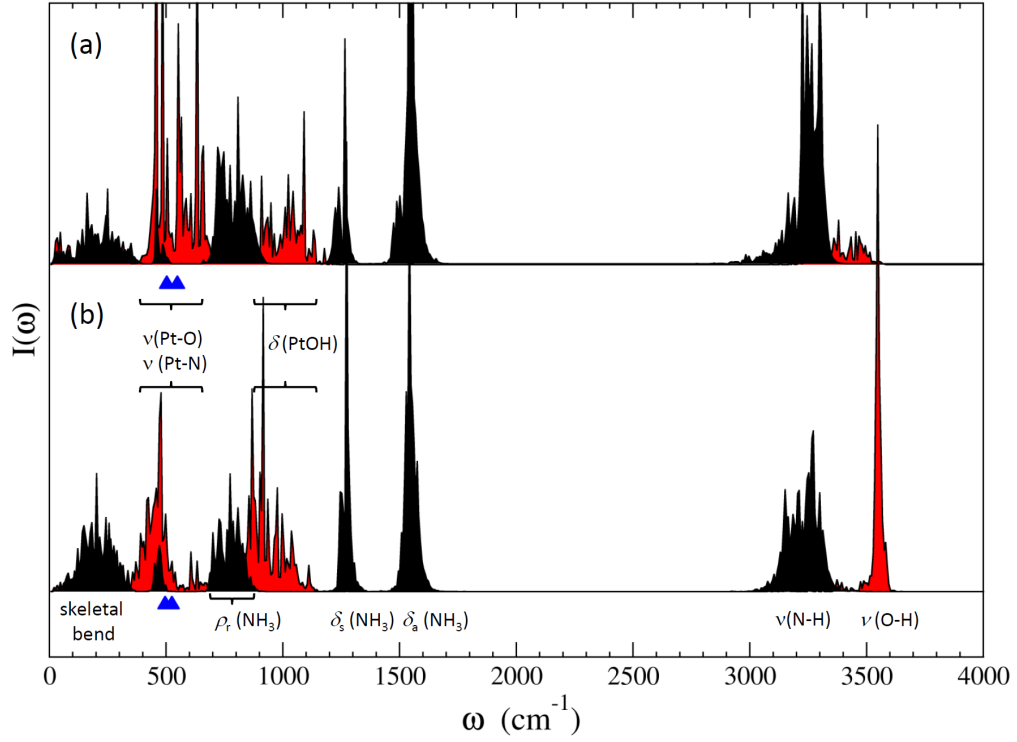


FIG. S3: CP-aiMD VDOS of the water-solvated (a) *cis*-Pt(NH<sub>3</sub>)<sub>2</sub>(OH)Cl and (b) *cis*-Pt(NH<sub>3</sub>)<sub>2</sub>(OH)<sub>2</sub> systems – both isolated from the bulk water. The total power spectrum has been deconvoluted in terms of NH<sub>3</sub> (in black) and OH (in red) vibrational contributions. The assignment of the vibrations is based on molecular quantum chemical calculations performed as part of this work. Selected experimental IR data<sup>8</sup> of solid *trans*-Pt(NH<sub>3</sub>)<sub>2</sub>(OH)<sub>2</sub> and *trans*-Pt(NH<sub>3</sub>)<sub>2</sub>(OH)Cl are also reported – the Pt–O and Pt–N stretching modes (blue triangles).



### S3. IMPLICIT TREATMENT OF THE SOLVENT EFFECTS

In order to investigate the reliability of an implicit treatment of the solvent effects, we have considered the conductor-like screening model (COSMO) as implemented self-consistently in ADF.<sup>9-11</sup> Among its semi-empirical parameters, the atomic radii used to construct the solute cavity are crucial.<sup>12-14</sup> Typically, the atomic radii are chosen to reproduce experimental solvation free energies<sup>15,16</sup> and not optimized for other properties. For H, N and O we have used the COSMO optimized radii ( $r_c$ ) of Ref. 11. For Cl and Br, we have chosen slightly increased Bondi van der Waals (vdW) radii<sup>17</sup> using  $r_c(\text{Cl}) = 1.8$  and  $r_c(\text{Br}) = 1.9$  Å.<sup>18</sup> The slope of the calculated <sup>195</sup>Pt isotropic shielding as a function of  $r_c(\text{Cl})$  and  $r_c(\text{Br})$ , i.e.  $\partial\sigma/\partial r_c$  at the vdW radius is around 1 ppm/pm for the square planar *cis*-Pt(NH<sub>3</sub>)<sub>2</sub>Cl<sub>2</sub> and *cis*-Pt(NH<sub>3</sub>)<sub>2</sub>Br<sub>2</sub> complexes (see Figure S4). A similar trend has been found for the oxygen atom in *cis*-Pt(NH<sub>3</sub>)<sub>2</sub>(OH)<sub>2</sub>. This effect is small compared to, for example, the influence of optimized and MD averaged Pt-ligand bond distances with  $\partial\sigma/R_{\text{PtX}}$  being on the order of 150 ppm/pm.<sup>19,20</sup> The COSMO radius of platinum has a somewhat larger influence. From the curves shown for the halide derivatives in Figure S4, we observe that: (i) for  $r_c(\text{Pt}) < 1.75$  Å,  $\partial\sigma/\partial r_c \approx 5$  ppm/pm ; (ii) for  $r_c(\text{Pt}) > 2.1$  Å,  $\partial\sigma/\partial r_c \approx 1$  ppm/pm ; (iii) for  $1.75 > r_c(\text{Pt}) > 2.1$  Å, the variation is very small. Thus, with a COSMO radius of less than the platinum vdW radius, the implicit solvent contributions are sensitive to the location of the COSMO surface charges, whereas for higher values  $r_c$  this effect is attenuated. For octahedral Pt complexes or more generally for complexes where the metal cannot be coordinated directly by the solvent these considerations do not apply. To our knowledge no optimization of the Pt radius, or more generally of transition metal radii, have been performed for polarizable continuum models for the purpose of NMR computations. Typically,  $r_c$  is similar to, or somewhat larger than, the vdW radius. In this work, we found that that a radius of 2.1 Å allows to reproduce quite well the explicit solvent effects (see main article) on the computed Pt shielding obtained from the aiMD averages.

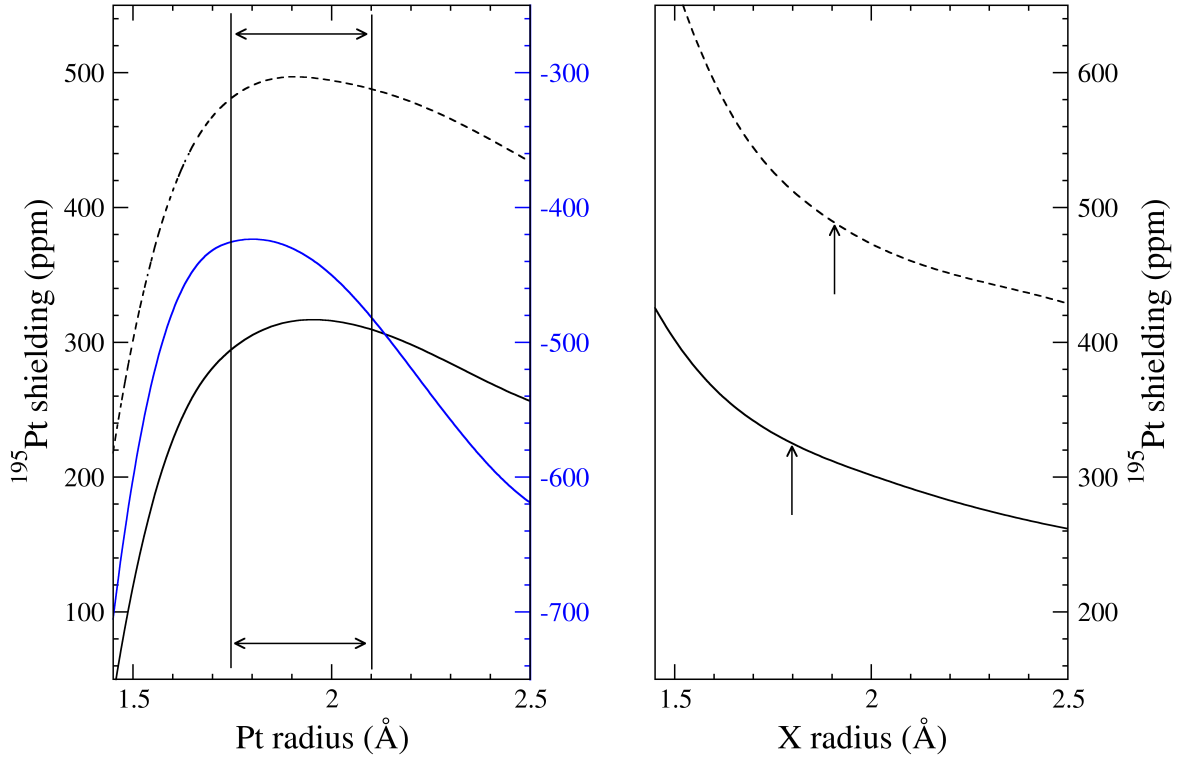


FIG. S4: Variation of the  $^{195}\text{Pt}$  isotropic shielding in the square planar complexes  $\text{cis-Pt}(\text{NH}_3)_2\text{Cl}_2$  (black plain line),  $\text{cis-Pt}(\text{NH}_3)_2\text{Br}_2$  (black dash line) and  $\text{cis-Pt}(\text{NH}_3)_2(\text{OH})_2$  (blue plain line) as a function of the atomic radii ( $r_c$ ) used in the COSMO-scalar-ZORA NMR calculations. Left panel: Pt radius influence (using  $r_c(\text{Cl}) = 1.8 \text{ \AA}$ ,  $r_c(\text{Br}) = 1.9 \text{ \AA}$ ,  $r_c(\text{O}) = 1.8 \text{ \AA}$ ). Right panel: Cl and Br radii influence (using  $r_c(\text{Pt}) = 2.1 \text{ \AA}$ ). The  $^{195}\text{Pt}$  isotropic shielding variation induced by the increase of the Pt radius from the Bondi's van der Waals value<sup>17</sup> ( $1.75 \text{ \AA}$ ) to the one used in this work ( $2.1 \text{ \AA}$ ) is described by horizontal arrows in the left panel. The Cl and Br radii used in this work are depicted by vertical arrows in the right panel.

#### S4. ENERGY PROFILE OF THE Pt...HOH INTERACTION

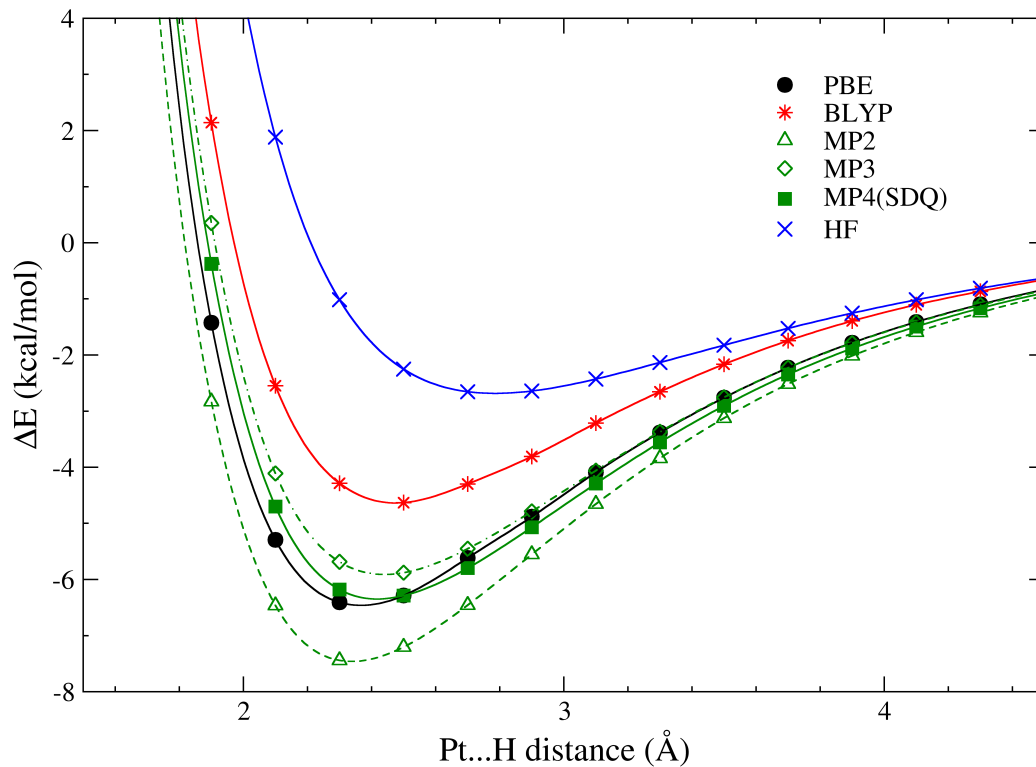


FIG. S5: Energy profiles along the Pt...H coordinate for cisplatin with one water molecule in the ‘H-ahead’ orientation. The energy scans were carried out with Gaussian 09.<sup>21</sup> Chlorine and platinum atoms were treated with the Los-Alamos effective core potentials,<sup>22,23</sup> along with the corresponding optimized basis sets,<sup>24</sup> including  $f$  and  $d$  polarization functions, respectively. The first row atoms were treated using all-electron double- $\zeta$  basis sets augmented with polarization and diffuse functions (6-31++G\*\*). The interaction energies were not corrected for basis set superposition errors.

- 
- <sup>1</sup> Lau, J. K.; Ensing, B. *Phys. Chem. Chem. Phys.* **2010**.
- <sup>2</sup> Carloni, P.; Sprik, M.; Andreoni, W. *J. Phys. Chem. B* **2000**, *104*, 823–835.
- <sup>3</sup> Fu, C.; Tian, S. X. *J. Chem. Phys.* **2010**, *132*, 174507.
- <sup>4</sup> Fedoce Lopes, J.; Ströele de A. Menezes, V.; Duarte, H. A.; Rocha, W. R.; De Almeida, W. B.; Dos Santos, H. F. *J. Phys. Chem. B* **2006**, *110*, 12047–12054.
- <sup>5</sup> Nakamoto, K.; McCarthy, P. J.; Fujita, J.; Condrate, R. A.; Behnke, G. T. *Inorg. Chem.* **1965**, *4*, 36–43.
- <sup>6</sup> Wysokiński, R.; Michalska, D. *J. Comput. Chem.* **2001**, *22*, 901–912.
- <sup>7</sup> Pavankumar, P. N. V.; Seetharamulu, P.; Yao, S.; Saxe, J. D.; Reddy, D. G.; Hausheer, F. H. *J. Comput. Chem.* **1999**, *20*, 365–382.
- <sup>8</sup> Arpalahiti, J.; Sillanpaa, R.; Barnham, K.; Sadler, P. *Acta Cryst. B* **1996**, *50*, 181–184.
- <sup>9</sup> Klamt, A.; Schüürmann, G. *J. Chem. Soc. Perkin Trans. 2* **1993**, 799–805.
- <sup>10</sup> Klamt, A. *J. Phys. Chem.* **1996**, *100*, 3349–3353.
- <sup>11</sup> Pye, C. C.; Ziegler, T. *Theor. Chem. Acc.* **1999**, *101*, 396–408.
- <sup>12</sup> Stefanovich, E. V.; Truong, T. N. *Chem. Phys. Lett.* **1995**, *244*, 65–74.
- <sup>13</sup> Cossi, M.; Barone, V.; Cammi, R.; Tomasi, J. *Chem. Phys. Lett.* **1996**, *255*, 327–335.
- <sup>14</sup> Chambers, C. C.; Hawkins, G. D.; Cramer, C. J.; Truhlar, D. G. *J. Phys. Chem.* **1996**, *100*, 16385–16398.
- <sup>15</sup> Sitkoff, D.; Sharp, K. A.; Honig, B. *J. Phys. Chem.* **1994**, *98*, 1978–1988.
- <sup>16</sup> Truong, T. N.; Stefanovich, E. V. *Chem. Phys. Lett.* **1995**, *240*, 253–260.
- <sup>17</sup> Bondi, A. *J. Chem. Phys.* **1964**, *68*, 441–451.
- <sup>18</sup> Marenich, A. V.; Cramer, C. J.; Truhlar, D. G. *J. Phys. Chem. B* **2009**, *113*, 6378–6396.
- <sup>19</sup> Truffandier, L. A.; Autschbach, J. *J. Am. Chem. Soc.* **2010**, *132*, 3472–3483.
- <sup>20</sup> Burger, M. R.; Kramer, J.; Chermette, H.; Koch, K. R. *Magn. Reson. Chem.* **2010**, in press.
- <sup>21</sup> Frisch, M. J. et al. *Gaussian 09, Revision A.02*; Gaussian, Inc., Wallingford, CT, 2009.
- <sup>22</sup> Hay, P. J.; Wadt, W. R. *J. Chem. Phys.* **1985**, *82*, 299.
- <sup>23</sup> Wadt, W. R.; Hay, P. J. *J. Chem. Phys.* **1985**, *82*, 284.
- <sup>24</sup> Roy, L. E.; Hay, P. J.; Martin, R. L. *J. Chem. Theory Comput.* **2008**, *4*, 1029–1031.